557396

Date: May 3, 2012

Sandia National Laboratories

Operated for the U.S. Department of Energy by the
Sandia Corporation
Defense Waste Management Programs
4100 National Parks Highway
Carlsbad, New Mexico 88220

To: WIPP Records Center

From: R. Chris Camphouse (6211)
Michael Gross, WTS Subcontractor
Courtney G. Herrick, Sandia National Labs (6211)
Dwayne C. Kicker, The S.M. Stoller Corporation
Bill Thompson, Golder Associates

Technical Review: Ross Kirkes

QA Review: Shelly Nielsen

Management Review: Janis Trone

Subject: Recommendations and Justifications of Parameter Values for the Run-of-Mine Salt Panel Closure System Design Modeled in the PCS-2012 PA

1.0 Introduction

The Waste Isolation Pilot Plant (WIPP), located in southeastern New Mexico, has been developed by the U.S. Department of Energy (DOE) for the geologic (deep underground) disposal of transuranic (TRU) waste. Containment of TRU waste at the WIPP is regulated by the U.S. Environmental Protection Agency (EPA) according to the regulations set forth in Title 40 of the Code of Federal Regulations (CFR), Part 191. The DOE demonstrates compliance with the containment requirements according to the Certification Criteria in Title 40 CFR Part 194 by means of performance assessment (PA) calculations performed by Sandia National Laboratories (SNL). WIPP PA calculations estimate the probability and consequence of potential radionuclide releases from the repository to the accessible environment for a regulatory period of 10,000 years after facility closure. The models used in PA are maintained and updated with new information as part of an ongoing process. Improved information regarding important WIPP features, events, and processes typically results in refinements and modifications to PA models and the parameters used in them. Planned changes to the repository and/or the components therein also result in updates to WIPP PA models. WIPP PA models are used to support the repository recertification process that occurs at five-year intervals following the receipt of the first waste shipment at the site in 1999.

WIPP waste panel closures comprise a feature of the repository that has been represented in WIPP PA regulatory compliance demonstration since the Compliance Certification Application (CCA) of 1996. Panel closures are included in the repository as a safety measure during the

operational period. In particular, their presence in the repository is a means to protect workers from exposure to two potential hazards: 1) volatile organic compounds that may be present in emplaced waste materials and 2) an explosion which has been hypothesized to occur from gas generation causing methane concentration in the waste panels to reach a sufficiently high level. Panel closures were not developed to isolate radionuclides in the repository after closure. The DOE stated in the CCA (DOE 1996) that *"The panel closure system was not designed or intended to support long-term repository performance."* Panel closures are included in WIPP PA models principally because they are part of the disposal system, not because they play a substantive role in inhibiting the release of radionuclides to the outside environment.

The WIPP was certified to receive TRU waste in 1998. The 1998 rulemaking had several conditions, one of which involved the design of the panel closure system (PCS) implemented in the repository. The DOE presented four design options in the CCA, and

> "The EPA based its certification decision on the condition that DOE implement the most robust design [referred to in the CCA as "Option D"]. The Agency found the Option D design to be adequate, but also determined that the use of a Salado Mass Concrete- using brine rather than fresh water- would produce concrete seal permeabilities in the repository more consistent with the values used in DOE's performance assessment. Therefore, Condition 1 of the EPA's certification requires DOE to implement the Option D PCS at the WIPP, with Salado Mass Concrete" (EPA 1998).

The Option D panel closure system consists of three primary components: 1) a concrete block wall (the explosion wall), 2) open drift, and 3) a concrete monolith. The arrangement and dimensions of these components are illustrated in Figure 1.

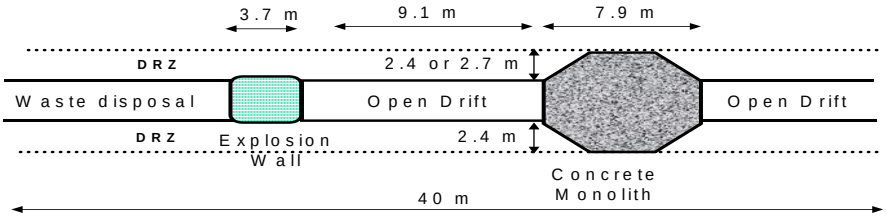

Figure 1: A Schematic of the "Option D" Panel Closure

Extensive refinement to WIPP panel closure modeling in PA has occurred since the implementation used in the CCA (Vugrin and Wagner 2006). In the CCA and the PAVT (MacKinnon and Freeze 1997) that followed, regulatory compliance was demonstrated with a generic panel closure that was not Option D. Following certification of the WIPP in 1998, and the mandate that Option D be implemented as the panel closure in WIPP, a PA was conducted in 2002 (Hansen 2002) with the aim of implementing an Option D panel closure into the repository

models used in WIPP PA, and to assess the impacts of panel closure design on long-term repository performance. Two panel closure cases were considered. The first was modeled upon the mandated Option D panel closure design. The second was the generic panel closure design implemented in the CCA and PAVT. Upon completion of the analysis, it was found that total normalized releases resulting from the two panel closure cases were nearly identical. Moreover, nearly identical distributions for each release component were calculated in the two panel closure cases. A more granular representation of the Option D panel closure was developed during the 2002 – 2003 Technical Baseline Migration (TBM) PA. Upon completion of the TBM PA, it was found that the TBM and PAVT produced releases that are nearly identical, indicating that repository performance is not significantly affected by changes in the panel closure properties (Dunagan 2003). The Option D panel closure representation developed during the TBM was used for the panel closure representation in the 2004 and 2009 Compliance Recertification Applications (CRA-2004 and CRA-2009, respectively).

Panel closures are represented in PA by way of their material properties and spatial extent. Due to the regulatory time scale of 10,000 years for which regulatory compliance must be demonstrated, there are uncertainties associated with panel closure material properties. These uncertainties in material properties are incorporated in PA. A material property with an associated uncertainty is assigned a distribution, and this distribution is randomly sampled. This sampling process allows for repository performance to be quantified over a range of material conditions, as well as an analysis of performance sensitivity to changes in material properties. As briefly described above, numerous studies have been conducted to date, often by way of full PA analyses, to quantify the impact of changes in panel closure material properties on regulatory compliance. In addition, several PA analyses have been performed (Hansen 2002, Vugrin & Dunagan 2006, Camphouse et al 2011) with the aim of determining the impact of panel closure redesigns on repository performance. Regulatory compliance has been met in all PA analyses performed to date, including those that incorporated changes to panel closure modeling. Regulatory compliance has been repeatedly shown to be primarily insensitive to panel closure material properties. A future PA is planned that incorporates a new panel closure design into the current PA baseline established by the 2009 Performance Assessment Baseline Calculation (PABC-2009) (Clayton et al., 2010). The name given to this planned panel closure PA is PCS-2012.

The PCS-2012 will quantify impacts of a run-of-mine (ROM) salt panel closure design by comparing total normalized releases to those found in the PABC-2009 where Option D was implemented as the panel closure. Calculations and analyses have been performed to develop material properties to be used in the PCS-2012, and are documented in DOE (2012) and Herrick (2012). This memorandum provides hydrologic and pore compressibility parameter values for the revised PCS in the PCS-2012 PA. Parameters are created as discussed in NP 9-2, *Parameters*. PCS-2012 parameters not listed in the memorandum will be equal to the values prescribed to them in the PABC-2009. In the discussion that follows, material parameters and timings are developed to account for the following physical processes and accepted rock mechanics principles:

1. Creep closure of the salt rock surrounding panel entries will cause consolidation of ROM salt emplaced in panel entries.

2. Eventually, the ROM salt comprising the closures will approach a condition similar to intact salt.
3. As ROM salt reaches higher fractional densities during consolidation, back stress will be imposed on the surrounding rock mass leading to eventual healing of the disturbed rock zone (DRZ).
4. DRZ healing above and below the ROM salt panel closures will reduce DRZ porosity and permeability in those areas.

A brief discussion of creep and reconsolidation of run-of-mine salt, and the DRZ healing that results, is the topic of the next section.

2.0 Creep and Reconsolidation of Run-of-Mine Salt

2.1 Creep Closure in Salt

The ability of salt to deform with time, eliminate voids, and create an impermeable salt barrier around the waste was one of the principal reasons for locating the WIPP repository in a bedded salt formation. The creep closure process is a complex and interdependent series of events starting after a region within the repository is excavated, which creates a disturbance in the stress field. Stress relief results in some degree of brittle fracturing and the formation of a DRZ surrounding excavations in all deep mines. For the WIPP, the DRZ is characterized by an increase in permeability, and may ultimately extend a few meters from the excavated region. Stress relief generates deviatoric stresses in the host rock, causing salt to deform by creep processes and to move inward to fill the excavated void. This process of salt creep will continue until deviatoric stress is dissipated and the system is once again at stress equilibrium (DOE 1996, Section 6.0.2.2 and Appendix PORSURF). Eventually, at equilibrium, deformation ceases, and the panel entry and any backfill (such as ROM salt) have undergone as much compaction as is possible by the weight of the rock above the repository horizon.

2.2 Mechanical Behavior of Run-of-Mine Salt

The mechanical behavior of ROM salt, which is also referred to as crushed salt, has been extensively studied and can be divided into three basic categories: elastic deformation, inelastic deformation, and failure (Callahan et al. 1995, Section 2.4.1). The inelastic behavior can further be divided into time-independent (instantaneous compaction) and time-dependent (creep consolidation) deformation. A number of parameters or characteristics are expected to affect the mechanical behavior of crushed salt. These parameters include (but are not limited to) density (or porosity), grain size and grain size distribution, moisture content, impurity content (such as clay, anhydrite, etc.), temperature, stress state (i.e., confining pressure and stress difference), and time.

Crushed salt is proposed as the main component of the redesigned panel closure, and over time this crushed salt will be consolidated by the creep closure of the entry. Crushed salt is also proposed as one component of the shaft seal, and an assessment of the mechanical behavior of crushed salt is provided as part of the WIPP shaft sealing system design (DOE 1996, Appendix SEAL). If salt reconsolidation is unimpeded by fluid pore pressures, the material will eventually achieve extremely low permeabilities approaching those of the native Salado Formation. Developments in support of the WIPP shaft seal system have produced confirming experimental results, constitutive material models, and construction methods that substantiate use of a salt

column to create a low permeability seal component. Other advantages of the use of crushed salt for sealing systems is that as a replacement of the natural material in its original setting it ensures physical, chemical, and mechanical compatibility with the host formation.

2.3 Response of the Disturbed Rock Zone

An underground excavation creates a disturbed zone in the surrounding rock. Microfracturing will occur in the rock adjacent to the drift wall, where confining stresses are low or nonexistent. The extent of the zone depends on the rock strength and the prevailing stress state, which is depth dependent.

In terms of WIPP repository applications, one of the most important features of salt as an isolation medium is its ability to heal previously damaged areas (Hansen 2003, Section 4.1). Damage recovery, or healing, arises when the magnitude of the deviatoric stress decreases relative to the applied mean stress. A decrease in deviatoric stress occurs as stresses approach lithostatic conditions, as would be the circumstance adjacent to the crushed salt barrier when it reaches a consolidated state. The healing mechanisms include microfracture closure and bonding of fracture surfaces. Microfracture closure is a mechanical response to increased compressive stress applied normal to the fractures, while bonding of fracture surfaces occurs either through crystal plasticity, a relatively slow process, or pressure solution and redeposition, a relatively rapid process (Spiers et al., 1988). Evidence for healing has been obtained in laboratory experiments, small-scale tests at WIPP and through observations of field analogs (Hansen 2003, Sections 4.5, 4.6, and 4.9).

2.4 Impact of ROM Salt Reconsolidation on Porosity and Permeability

Numerical modeling conducted as part of shaft sealing analyses provides density of the compacted salt column as a function of depth and time. Many calculations comparing models for consolidation of crushed salt were performed to quantify performance of the crushed salt column in the shaft seal (DOE 1996, Appendix SEAL; Callahan et al. 1995; Brodsky et al. 1996). From the density-permeability relationship of reconsolidating crushed salt, permeability of the compacted salt seal component is calculated. In general, results show that the bottom of the salt column consolidates rapidly, achieving permeability of 1×10^{-19} m^2 in about 50 years. By 100 years, the middle of the salt column reaches similar permeability.

Structural analysis calculations were developed to determine the fractional density of the crushed salt seal as a function of time and depth and, using these results, to determine permeability of the crushed salt as a function of time and depth (DOE 1996, Appendix SEAL, Section 7.4.2.1). The results of these calculations indicate that compacted salt will increase from its emplaced fractional density of 90% to a density of 95% approximately 40, 80, and 120 years after emplacement at the bottom, middle, and top of the shaft seal, respectively. Using the modified Sjaardema-Krieg creep consolidation model, the times required to fully reconsolidate the crushed salt to 100% fractional density are 70 years, 140 years, and 325 years at the bottom, middle, and top of the salt column, respectively. Based on these results, the desired fractional densities (hence, permeability) can be achieved over a substantial length of the compacted salt seal in the range of 50 to 100 years.

Additional details on the porosity and permeability of ROM salt are provided in Sections 5.1.1 and 5.1.2. Based on the calculations cited above and on in situ observations as described in Section 5.1.1, it is expected that a completely consolidated ROM salt-filled drift will achieve flow properties indistinguishable from natural Salado salt. The ability of salt to recover from damage and heal is a time-dependent process; eventually, the permeability of the consolidated ROM salt and the surrounding DRZ will return to that of intact salt.

3.0 Revised Design of the PCS

The DOE has submitted a planned change request (PCR) to the EPA requesting that EPA modify Condition 1 of the Final Certification Rulemaking for 40 CFR Part 194 (EPA, 1998) for the WIPP. Following the selection of the Option D panel closure design in 1998, the DOE has reassessed the engineering of the panel closure and established a revised design which is simpler, easier to construct and equally effective at performing its operational-period isolating function. Accordingly, the PCR submitted to EPA requested that Condition 1 be changed, and that a revised design for the panel closures be approved for use in all panels (DOE, 2011). The revised design of the PCS, known as the Run-of-Mine Panel Closure System (ROMPCS), comprises 100 feet of run-of-mine (ROM) salt with barriers at each end (Figure 2). The ROM salt is generated from ongoing mining operations at the WIPP and may be compacted and/or moistened as it is emplaced in a panel entry. The ROM salt will be emplaced to all salt surfaces (back, walls, etc.) as completely as practicable. After emplacement, creep closure of the panel entries will cause the ROM salt to consolidate to a condition approaching intact salt, with low porosity and low permeability.

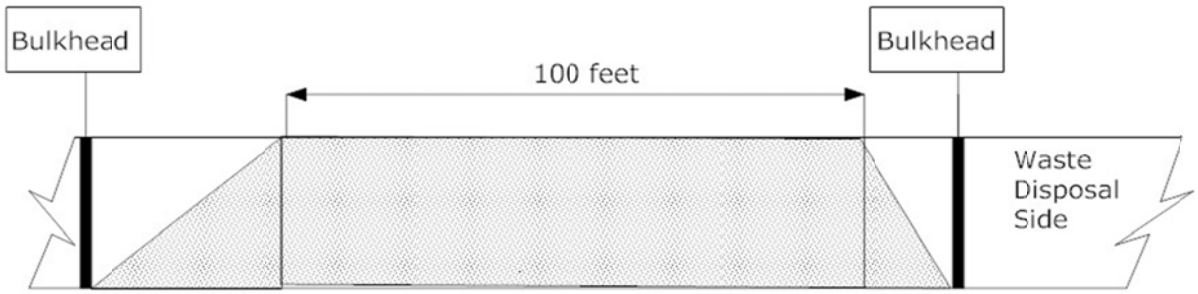

(a) Panel closure with 100 feet of ROM salt between two ventilation bulkheads

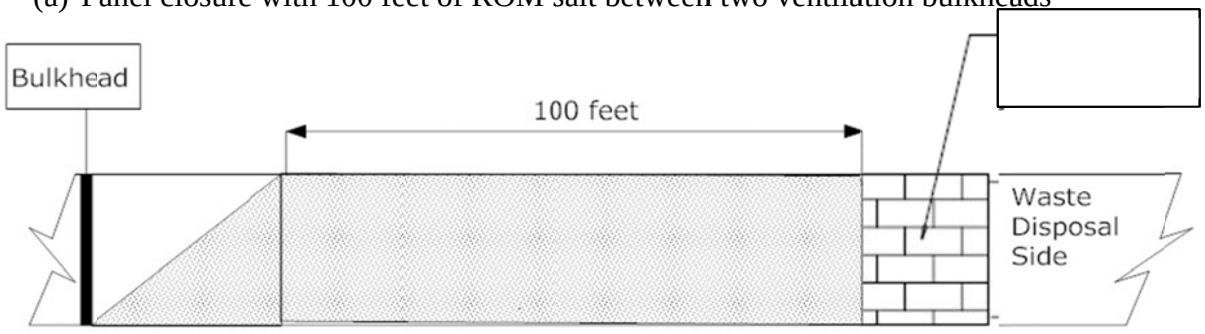

(b) Panel closure with 100 feet of ROM salt between a ventilation bulkhead & explosion wall

Figure 2. Schematic diagram of the revised panel closure design

The barriers will consist of ventilation bulkheads, similar to those currently used in the panels as room closures (Figure 3). The ventilation bulkheads are designed to restrict air flows and prevent personnel access into waste-filled areas during the operational phase. In Panels 1, 2, and 5, where explosion walls fabricated from concrete blocks have already been emplaced in the panel entries, an explosion wall is the inbye barrier and a ventilation bulkhead will be the outbye barrier, as shown in Figure 2b.

The emplacement scheme for the ROM salt will be finalized once *in situ* testing has been completed. It is expected that the final emplacement scheme will involve some degree of in-place compaction, with or without added moisture (moisture may be added because it accelerates the consolidation of the crushed salt). The emplacement technique and/or strategy *is not* important to long-term repository performance. In particular, the uncertainty in the final panel closure emplacement strategy is not a result of consideration of long-term panel closure characteristics. Panel closures are emplaced in the repository to protect workers during the operational phase of the facility. Emplacement uncertainty is due to current lack of operational experience in constructing/emplacing this type of closure system. The method used will be based on consideration of various operational variables. Cost, efficiency, short-term effectiveness, dust control, and other factors will all play into the final emplacement scheme. A range of possible emplacement strategies are being assumed in the PCS-2012 to develop panel closure materials, properties, and timings representative of all potential emplacement strategies.

At one end of the range is emplacement of dry ROM salt without any initial compaction. The uncompacted porosity of ROM salt is assumed to be 35%, based on several sources. Callahan and Devries (1991, Section 4.1 and Table 2-2) define the initial density of crushed salt as about 65% of intact density, based on data from (Sjaardema and Krieg, 1987) and (Weatherby, 1989). This initial density corresponds to an initial porosity of approximately 35% for the crushed salt. Recent work on backfill compaction in the German repository program also assumes an initial backfill porosity of 35% (Rothfuchs and Wieczorek, 2010). The uncompacted ROM salt is therefore assumed to have an initial porosity of 35%, equivalent to a fractional density of 65%. At the other extreme, the ROM salt may be emplaced in compacted layers that are wetted with a small amount of moisture to enhance the initial emplacement density and short-term consolidation. The average porosity of the compacted layers is estimated to be greater than 20%, based on engineering judgment. The values of the hydrologic and mechanical parameters for the PCS-2012 PA are intended to encompass both of these extremes.

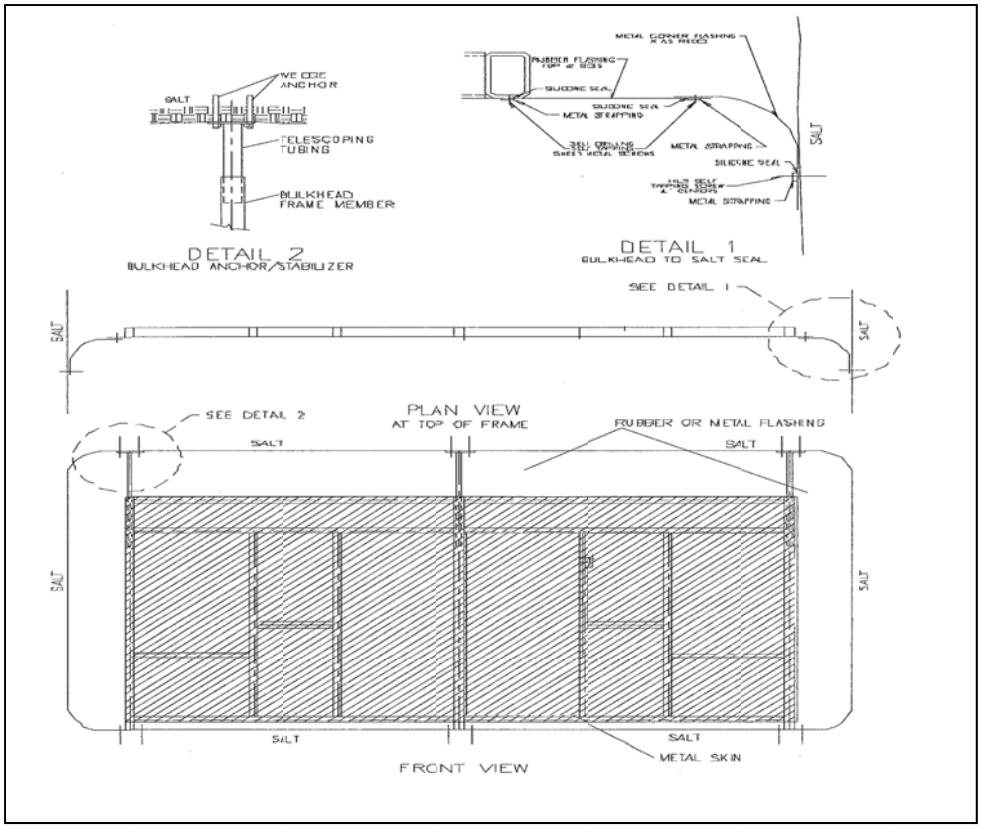

Figure 3. Typical design of a ventilation bulkhead that blocks the panel entry

The ROM salt is chemically compatible with the host rock because it is mined from the host rock at the repository horizon and because it has no additives, except for the possible addition of a small amount of moisture. The sheet metal in the ventilation bulkhead has small mass and is chemically similar to the iron-based metals in the waste and waste containers that are already in the repository. The materials in the redesigned PCS will therefore be chemically compatible with the host rock and with the materials already in the repository.

4.0 Modeling Approach for PCS-2012 PA

A new PA baseline was established by the PABC-2009 (Clayton et al., 2010). The differences between the PABC-2009 and the PCS-2012 PA will be a direct consequence of the revised design of the PCS. More specifically, the PCS-2012 PA will use the BRAGFLO grid that was used for the PABC-2009, but with new properties for the materials that represent the ROM salt in the PCS and the disturbed rock zone directly around the PCS. Note that the Option D panel closure implemented in the PABC-2009 is 40 meters long (Figure 1) while the redesigned PCS modeled in the PCS-2012 is 100 feet (30.48 meters) long. The PABC-2009 BRAGFLO grid will be modified slightly to account for the reduction in length of the ROMPCS as compared to Option D.

The ROMPCS properties will be based on three time periods: from 0 to 100 years, from 100 years to 200 years, and from 200 years to 10,000 years. This is a refinement to the granularity of panel closure modeling undertaken in the 2006 PCS PA (Vugrin and Dunagan 2006) and the

2011 PC3R PA (Camphouse et al 2011). Three time periods are appropriate because the process to consolidate the ROM salt occurs over a primary time scale of approximately 100 years, while the process to heal fractures in the DRZ surrounding the PCS occurs over a longer time scale of approximately 200 years. The ROM salt will therefore be represented by three materials, denoted as PCS_T1 for the first 100 years, PCS_T2 for 100 to 200 years, and PCS_T3 for 200 to 10,000 years. Similarly, the DRZ directly above and below the ROM salt will be represented by materials DRZ_PCS_T1, DRZ_PCS_T2, and DRZ_PCS_T3.

The ventilation bulkheads are designed to provide isolation only during the operational period. These bulkheads are not expected to remain intact 100 years after repository closure because of creep closure of the panel entries. The explosion wall is also designed for the operational period. This wall is inspected on a regular basis, and the anticipated condition of the wall is also assessed through numerical modeling (e.g. RockSol, 2006). Figures 4 and 5 present photographs of the condition of the free face in Panel 1 during February 2012. The explosion wall shows surface spalling or slabbing of the concrete blocks as a result of the loading caused by inward creep of the salt. In contrast, the plastic properties on the ROMPCS will allow it to reconsolidate and heal under increasing load due to salt creep. The thickness of the slabs shown in Figure 4 is typically 1.2 to 1.5 inches and quite consistent. The rod in Figure 5 is anchored by a nut resting on a thin layer of bricks that have become detached and pushed out by the formation of a crack about an inch behind the free surface.

Figure 4. Surface spalling at the base of the explosion wall in the intake drift of Panel 1 during February 2012

Figure 5. Surface spalling at the top corner of the explosion wall in the intake drift of Panel 1 during February 2012.

Numerical stress analysis of the concrete explosion wall has demonstrated that the free faces and the rib contacts will be in a condition of plastic yield with an unyielded core by 7 years after emplacement (Rocksol, 2006, Figures 7 and 10). No long term stress analyses have been carried out; however, it is expected that the spalling and yield will be progressive, and that the walls will not be significant structures after the initial 100 year time period, due to the brittle, non-plastic behavior of concrete. The ventilation bulkheads and explosion walls will therefore have no significant impact on long-term performance of the panel closures and are not included in the analysis of material properties for the PCS and the DRZ surrounding the PCS. Additionally, during the initial 100 year period after repository closure, the primary potential flow path through the closure system will be through the DRZ so any influence from the bulkheads or explosion wall will be minimal.

5.0 PCS Parameters

As discussed in Section 2.0, the salt rock surrounding the panel entries is creeping closed, and this closure will cause consolidation of ROM salt emplaced in panel entries. Eventually the ROM salt will approach a condition equivalent to intact salt. During the consolidation process, as the ROM salt reaches higher fractional densities, a back stress will be imposed on the surrounding rock mass leading to healing of the DRZ and a reduction in DRZ porosity and permeability. These processes and their effect on porosity and permeability of the ROM salt and the surrounding DRZ are discussed in Section 2.0. This section of this memorandum provides values for a complete set of hydrologic parameters and the pore compressibility parameter for the ROM salt and for the DRZ directly above and below the PCS.

5.1 Hydrologic and Pore Compressibility Parameters for the ROM Salt

5.1.1 Porosity of ROM Salt

Estimates of the consolidation process have been made in a series of calculations (Herrick 2012) carried out using JAS3D (Blanford et al., 2001; DOE, 2012, Figures 4 through 7) with the Sjaardema and Krieg (1987) model for crushed salt, modified with a deviatoric creep compaction response (Stone, 1997). Separate calculations were performed for initial emplacement porosities of 20%, 25%, 30%, and 35%, which correspond to initial fractional densities of 80%, 75%, 70%, and 65%, respectively. These calculations show consolidation to a porosity of 5% in 65 years from an initial porosity of 20% and in 152 years from an initial porosity of 35%. The results from the JAS3D calculations during the first 150 years are summarized in Table 1 as a function of time and initial emplacement porosity.

Table 1. Porosity predicted by JAS3D for ROM salt in a panel entry as a function of time and initial emplacement porosity

Time After Emplacement (Years)	Porosity			
0	20%	25%	30%	35%
50	6.6%	10.3%	14.6%	18.7%
100	1.9%	4.2%	7.3%	10.7%
150	1.0%	1.2%	2.9%	5.2%

During the first time period, from 0 to 100 years, the data in Table 1 show that the porosity of the ROM salt decreases rapidly. In order to represent this time varying porosity in a way suitable for long-term performance assessment calculations, it is reasonable to define the range of porosity of the ROM salt at the midpoint of this time interval, 50 years. The porosity range for the first 100 years is then 6.6% to 18.7%, based on the second row of data in Table 1. This range explicitly accounts for the uncertainty in initial emplacement porosity for the ROM salt.

For the time period from 100 to 200 years, the porosity range is 2.5% to 7.5%, with an expected or mean porosity of 5%. The lower limit for the porosity range, 2.5%, is essentially the same as the lower limit of porosity from the JAS3D calculations at 100 years, 1.9% (see Table 1). The upper limit for the porosity range, 7.5%, is less than the maximum porosity from the JAS3D calculations at 100 years, which is 10.7% (see Table 1); however, the JAS3D calculation for ROM salt with an initial porosity of 35% predicts a porosity of 7.5% by 126 years after emplacement. The value of 7.5% as an upper limit is also consistent with the magnitude of the porosity range for intact halite. That is, the magnitude of the porosity range from 100 to 200 years is 7.5% - 2.5% = 5%, approximately equal to the magnitude of the observed porosity range for intact salt, which is 5.19% - 0.1% = 5.09% (DOE 2009, Appendix PA, Parameter 17; Ismail 2007). Finally, the mean porosity, 5%, is consistent with the JAS3D predictions at 100 years, which have a porosity range of 1.9% to 10.7% at 100 years after emplacement (see the 3rd row of data in Table 1).

A number of sources corroborate the use of a reduced upper limit, 7.5% rather than 10.7%, during the second time period. Hurtado et al. (1997) carried out a number of consolidation

estimates for the proposed crushed salt component of the shaft seals. The proposed crushed salt component of the shaft seals will consist of mined WIPP crushed salt, dynamically precompacted with added moisture to a porosity of 10%. Calculations of the consolidation of this component due to creep closure of the shaft indicate that the crushed salt will be at an essentially intact condition (a fractional density approaching 1) within 100 years at a depth of 515 m and within 60 years at a depth of 600 m (Hurtado et al. 1997, Figure 2-3). Additional calculations by Callahan (1999) show consolidation results for different crushed salt models at depths of 430 m, 515 m, and 600 m, indicating similar results to Hurtado et al. (1997). Callahan and DeVries (1991) conducted calculations on the closure of disposal rooms backfilled with crushed salt that show closure to essentially intact density in about 25 years. Collectively, these alternate calculations imply that a mean porosity of 5% and an upper limit of 7.5% by 100 years after emplacement are reasonable and conservative values.

The consolidation process will continue after 200 years, particularly for ROM salt that is emplaced dry with minimal compaction. This is accounted for by assigning a third time period, 200 to 10,000 years, during which consolidation of the ROM salt will continue and achieve a porosity similar to that of intact salt regardless of the emplacement strategy. *In situ* observations from the BAMBUS II project at the Sigmundshall mine in Germany indicate consolidation of a crushed salt slurry to essentially an intact condition within tens of years (Bechthold et al., 2004, Figure 2.57). Consolidation to an essentially intact condition is also confirmed by observations at the Rocanville mine, where a consolidated salt plug was emplaced after a water inflow, and has been effective in sealing off a hydrostatic groundwater pressure of about 1200 psi (8.3 MPa) (Van Sambeek et al., 1995). The state of the intact halite at WIPP therefore provides an analog for the long-term consolidated state of ROM salt in a panel entry. Table 2 summarizes the values for porosity of the ROM salt as a function of time.

The values in Table 2 indicate that there is a significant overlap between the porosity ranges for the 100 to 200 year and the 200 to 10,000 year time periods. More specifically, the 2.5% to 5.19% porosity range is included in both time periods, although this range represents the lower end of the porosity range from 100 to 200 years and the upper end of the porosity range from 200 to 10,000 years. This representation is very reasonable because the consolidation process will continue after 200 years, particularly for ROM salt that is emplaced with minimal compaction, and because the JAS3D predictions show that the rate of consolidation decreases significantly after 100 years, making an overlap in the porosity range likely to occur as porosity decreases to *in situ* values.

Table 2. Porosity of the ROM salt during three time periods

Parameter	Time Period	Assumed Porosity	Notes
PCS_T1:POROSITY	0 to 100 years	6.6% to 18.7%	Assumes ROM salt is emplaced with an initial porosity of 20% to 35%. An initial porosity of 35% represents no compaction during emplacement.
PCS_T2:POROSITY	100 to 200 yrs	2.5% to 7.5%	2.5% to 7.5% is consistent with the JAS3D calculations and is conservative relative to alternate computational predictions from several sources.
PCS_T3:POROSITY	200 to 10,000 yrs	0.1% to 5.19%	Assumes that the porosity of crushed salt after 200 years is equal to the porosity for intact halite.

5.1.2 Permeability of ROM Salt

Laboratory experiments on consolidated cores of crushed salt confirm that the intrinsic permeability of crushed salt decreases as the fractional density of the cores increases (Hurtado et al. 1997, Figure 2-1). This observation is corroborated by other experiments on the behavior of crushed salt under similar conditions to WIPP (Case et al., 1987; Zhang et al., 2007); although the cores tested by Zhang et al. (2007) are for salt from the Asse mine and some of the core tested by Case et al. (1987) is for salt from Avery Island, the overall behavior of the crushed material is expected to be similar. The general observations from testing of crushed salt cores are that: (1) intrinsic permeability decreases as the fractional density increases (or as the porosity decreases), (2) crushed salt cores with added moisture generally have lower values of intrinsic permeability than dry cores, and (3) cores of crushed salt with smaller grain sizes generally have lower values of intrinsic permeability than cores with larger grain sizes. The first and third observations are generally valid for all granular materials, while the second observation specifically relates to the microstructure of the salt cores and requires further explanation.

At equivalent fractional densities, dry consolidated salt cores are more permeable than wet consolidated salt cores because of the difference in the mechanism causing consolidation. Under dry conditions, the effective consolidation mechanism is crystal plasticity, while under wet conditions the effective consolidation mechanism is pressure solution/redeposition (Hurtado et al. 1997, page 2-7; Case et al., 1987, Section 4). Pressure solution/redeposition under wet conditions generally produces higher consolidation rates and more deformation than crystal plasticity under dry conditions, leading to lower measured permeability for wet consolidated salt than for dry consolidated salt at equivalent fractional densities (Hurtado et al. 1997, Figure 2-1; Case et al., 1987, data for Test 3 in Figure 1).

During the first time period, from 0 to 100 years, the porosity of the ROM salt varies from 6.6% to 18.7% (see Table 2). Table 3 summarizes permeability data for cores of crushed salt that are relevant to the maximum porosity of 18.7%. The data are from three sources: Hurtado et al. (1997), Case et al. (1987), and Zhang et al. (2007). Hurtado et al. (1997) summarizes data from (Brodsky 1994) and (Brodsky et al., 1996) for wet and dry cores, respectively. The permeability data from the three sources are remarkably consistent and provide a basis for defining the maximum permeability as approximately 10^{-12} m^2 at a porosity of 18.7%.

Table 3. Permeability data for cores of crushed salt at 18.7% porosity

Source	Porosity	Permeability (m^2)	Notes
(Brodsky et al., 1996), summarized in Table 2-1 of (Hurtado et al., 1997)	17.8%	4.11×10^{-13} m^2	For dry WIPP salt at fractional density of 0.822 (porosity of 17.8%). This core has the greatest porosity of the data in (Brodsky et al., 1996) and (Brodsky 1994).
Case et al., 1987, Figure 1	18.7%	1×10^{-13} m^2 to 2×10^{-12} m^2	For dry WIPP salt with 0.9 mm and 10 mm maximum grain sizes (Tests 1 and 2) and for moistened WIPP salt with 20 mm maximum grain size (Test 3).
Zhang et al., 2007, Figure 4	18.7%	2×10^{-13} m^2 to 1×10^{-12} m^2	For dry Asse salt cores with maximum grain size of 32 mm.

At the minimum porosity value of 6.6% during the first 100 years after facility closure, the measurements have a wide range of permeability because of the microstructure of the cores. Table 4 has the measured values that are relevant to a porosity of 6.6%. The gas permeability data for dry cores at 6.6% are relatively consistent from the three sources, falling within a permeability range of 10^{-15} m^2 to 10^{-14} m^2. The brine permeability from Case et al. (1987) is lower than the brine permeability from Hurtado (1994), which may be caused by the maximum grain size for the cores. Test 3 from Case et al. (1987, Table 1) has a maximum grain size of 20 mm, while the maximum grain size of ROM WIPP salt was measured at 1.5 inches (38 mm) (Pettigrew and Associates, 1993), or almost twice as large as the crushed salt for Test 3. Cores with finer grain sizes are expected to have lower permeability than cores with larger grain sizes, which may explain the observed difference in permeability from different sources.

Table 4. Permeability data* for cores of crushed salt at 18.7% porosity

Source	Porosity	Permeability (m^2)	Notes
(Brodsky et al., 1996) & (Brodsky, 1994), summarized in Table 2-1 of (Hurtado et al., 1997)	6.61%	4.95×10^{-15} m^2	For dry WIPP salt at a fractional density of 0.9339 (porosity of 6.61%)(Brodsky et al., 1996)
	6.67%	2.14×10^{-19} m^2	For wet WIPP salt at a fractional density of 0.9333 (porosity of 6.67%)(Brodsky 1994)
Case et al., 1987, Figure 1	6.6%	1×10^{-15} m^2 to 1×10^{-14} m^2	For dry WIPP salt with 0.9 mm and 10 mm maximum grain sizes (Test 1 and Test 2)
	6.6%	1×10^{-21} m^2 to 1×10^{-20} m^2	For wet WIPP salt with 20 mm maximum grain size (Test 3).
Zhang et al., 2007, Figure 4	18.7%	1×10^{-14} m^2	For dry Asse salt cores with maximum grain size of 8 mm.

*Data on fractional density and permeability from (Brodsky, 1994) and (Brodsky et al., 1996) are reproduced with the same number of digits in (Hurtado et al., 1997, Table 2-1) to facilitate identification of specific measurements in the data sets.

The range of permeability for performance assessment should encompass the range of laboratory measurements shown in Tables 3 and 4. At a porosity of 18.7%, the maximum permeability is approximately 10^{-12} m^2. At a porosity of 6.6%, the brine permeability from Hurtado et al. (1997) is about 2×10^{-19} m^2. The brine permeability data from Case et al. (1987) are not used here because the maximum grain size for Test 3, 20 mm, is somewhat smaller than the measured maximum grain size for WIPP salt, 38 mm. We therefore determine that the permeability of the ROM salt should be sampled from a log-uniform distribution, [2×10^{-19} m^2, 10^{-12} m^2], during the first time period, from 0 to 100 years.

During the second and third time periods, the permeability of consolidated ROM salt is based on the experimental measurements of consolidated WIPP salt cores summarized in Hurtado et al. (1997) and further documented in additional Sandia documents (Brodsky, 1994; Brodsky et al., 1996; Ahrens and Hansen, 1995). This analysis uses the brine permeability data from Brodsky (1994) for two reasons. First, the salt cores are based on ROM salt from the WIPP and provide a consistent data set for defining permeability as a function of porosity. Second, the fractional densities of the salt cores measured by Brodsky (1994) have a range of 0.8953 to 1.0051[1] (porosity of 10.47% to ~ 0%, resp.), which encompass the porosity range of interest during the second and third time periods (see Table 2). The alternate data sets are either sparsely populated

[1] A fractional density greater than 1 may imply uncertainty in the assumed density of intact salt.

at the porosities of interest during the second and third time periods or are based on crushed salt with finer grain sizes than ROM salt from the WIPP.

The permeability data from Brodsky (1994) are represented as a function of porosity through a two-step relationship: (1) a least squares fit to the permeability data as a function of fractional density, and (2) a normal distribution that represents the residuals of the data about the least squares fit. This approach captures the mean variability of permeability with porosity and represents the uncertainty in the data set. Figure 6 shows the least squares fit to the data from (Brodsky, 1994). Figure 7 is a quantile-quantile plot showing that a normal distribution provides a good representation of the residuals of the individual data points about the least squares fit. (The closeness of the individual points to the straight line in Figure 7 indicates the goodness of fit by a normal distribution.) This normal distribution has a mean of 0.0 and a standard deviation of 0.86. The parameters for the normal distribution are determined by the data, without adjustment or expert judgment. Given the limited number of data points from Brodsky (1994), the normal distribution will be truncated at plus or minus two standard deviations.

The relationship between porosity and permeability can be mathematically written as:

$$\log(k_e) = -21.187(1-\phi) + 1.5353, \quad (1)$$

$$k = 10^{\log(k_e)+\alpha} = k_e 10^{\alpha}, \quad (2)$$

where k_e is the expected value of permeability from the least squares fit,
ϕ is the sampled value of porosity,
k is the final value of permeability, and
α is the sampled value of a normal distribution with a mean of 0, a standard deviation of 0.86, and truncated at ±2 standard deviations.

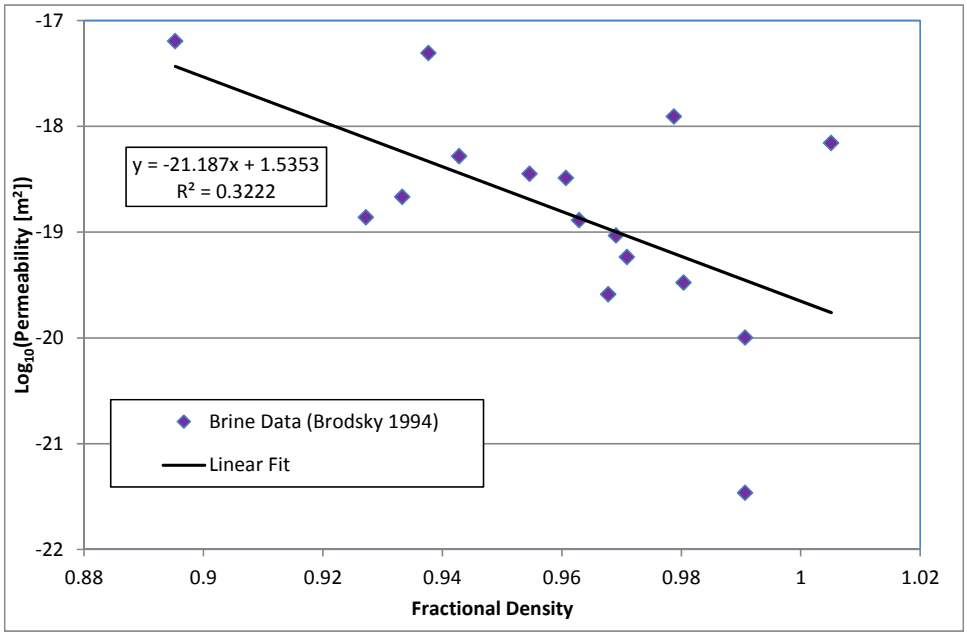

Figure 6. Least squares fit to brine permeability measurements for WIPP crushed salt

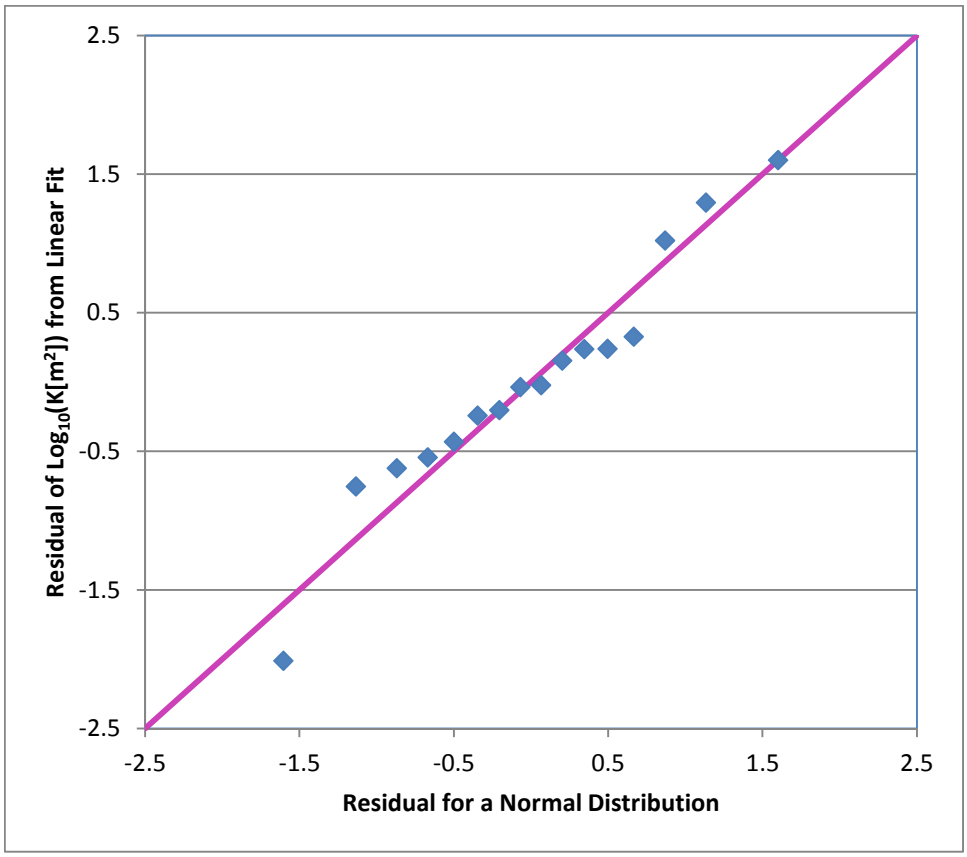

Figure 7. Quantile-quantile plot of the data residuals relative to the linear fit and of the predicted residuals for a normal distribution with mean of 0.0 and standard deviation of 0.86

The following algorithm for representing the values of PCS_T1:PRMX_LOG, PCS_T2:PRMX_LOG and PCS_T3:PRMX_LOG in PA should be used:

1. The value of PCS_T1:POROSITY is sampled from a uniform distribution, [6.6%, 18.7%], in each realization.
2. The permeability [m^2] of ROM salt from 0 to 100 years, PCS_T1:PRMX, is sampled from a log-uniform distribution, [2×10^{-19} m^2, 10^{-12} m^2], in each realization. The values of PCS_T1:PRMY and PCS_T1:PRMZ are set equal to PCS_T1:PRMX.
3. For each realization, the value for PCS_T2:POROSITY between 100 and 200 years is sampled from a uniform distribution with a minimum of 0.025 and a maximum of 0.075. The value for PCS_T3:POROSITY between 200 and 10,000 years is sampled from a uniform distribution with a minimum of 0.001 and a maximum of 0.0519.
4. Calculate the expected values of the $\log_{10}(k_e)$, the logarithm of the expected permeability, using Equation (1) with the sampled values of PCS_T2:POROSITY and PCS_T3:POROSITY.
5. Sample a normal distribution (mean of zero, standard deviation of 0.86) that is truncated at ±2 standard deviations and calculate the final value of the permeability, k, using Equation (2). This calculation is performed twice, once for 100 to 200 years, and a second time for 200 to 10,000 years. This sampling is performed once per realization.

6. The values of PCS_T2:PRMX, PCS_T2:PRMY, and PCS_T2:PRMZ are set equal to the value of k for the second time period. The values of PCS_T3:PRMX, PCS_T3:PRMY, and PCS_T3:PRMZ are set equal to the value of k for the 200 to 10,000 year time period.

Figure 8 shows the range of permeability as a function of fractional density for this algorithm. Table 5 presents numerical values of the minimum, and maximum permeability from 0 to 100 years, from 100 to 200 years, and from 200 to 10,000 years based on this approach. For the latter two time periods, the mean permeability is based on the sampled value of porosity (between 0.025 and 0.075 for 100 to 200 years, and between 0.001 and 0.0519 for 200 to 10,000 years), as defined by the least squares fit (Equation (1)). The minimum and maximum permeability values correspond to -2 and +2 standard deviations on the normal distribution, respectively (Equation (2)).

The 2.5% to 5.19% porosity range is included in both the 100 to 200 year and the 200 to 10,000 year time periods (see discussion in Section 5.1.1), and represents the lower end of the porosity range from 100 to 200 years and the upper end of the porosity range from 200 to 10,000 years. This provides an overlap in the permeability ranges for these two time periods, although the effect is mitigated by sampling the uncertainty in the data about the least squares fit in Figure 8.

With this algorithm, the calculated permeability value for 200 to 10,000 years may be greater than the calculated permeability value for 100 to 200 years. This is not a reasonable outcome, so the permeability value for 200 to 10,000 years should be sampled so that it is never greater than the permeability value for 100 to 200 years.

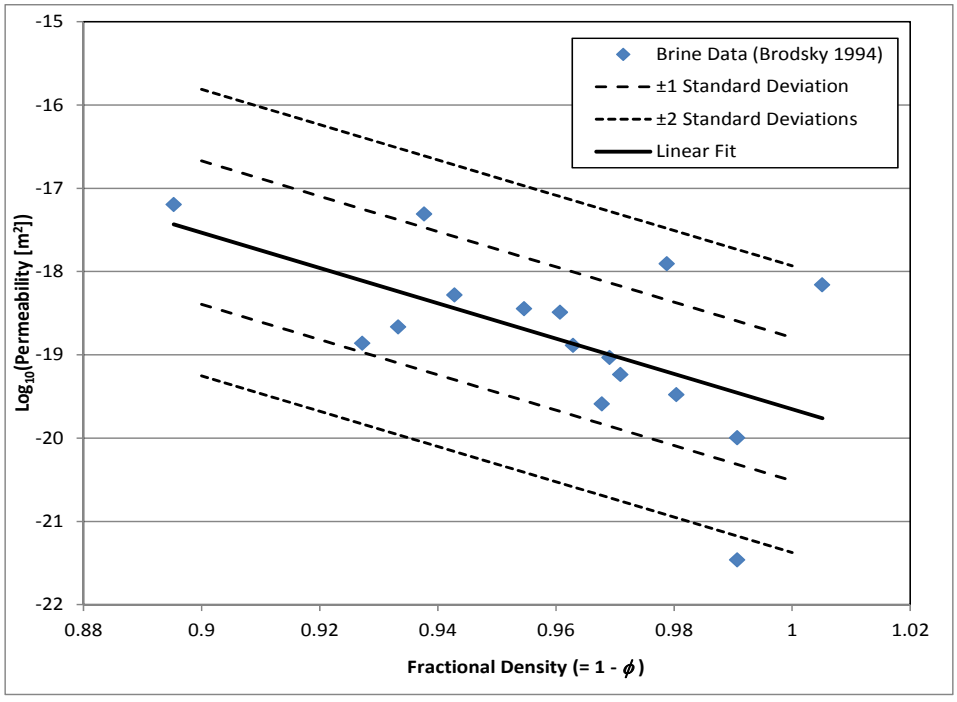

Figure 8. Variation of permeability with fractional density, based on the least squares fit and a normal distribution with a mean of 0.0 and a standard deviation of 0.86

Table 5. Permeability of the ROM salt during three time periods

Parameter(s)	Porosity	Fractional Density	Minimum[a,b] Permeability	Maximum[a,b] Permeability
PCS_T1: PRMX_LOG, PRMY_LOG, PRMZ_LOG	6.6% to 18.7%	0.825 to 0.933	-18.7 (2×10^{-19} m^2)	-12 (1×10^{-12} m^2)
PCS_T2: PRMX_LOG, PRMY_LOG, PRMZ_LOG	0.025	0.975	-20.8 (1.44×10^{-21})	-17.4 (3.96×10^{-18})
	0.075	0.925	-19.8 (1.65×10^{-20})	-16.3 (4.55×10^{-17})
PCS_T3: PRMX_LOG, PRMY_LOG, PRMZ_LOG	0.001	0.999	-21.4 (4.46×10^{-22})	-17.9 (1.23×10^{-18})
	0.0519	0.9481	-20.3 (5.34×10^{-21})	-16.8 (1.47×10^{-17})

[a] Each cell has the log(k[m^2]) and the corresponding value of k in parentheses.
[b] Minimum corresponds to -2 standard deviations below the least squares fit; maximum corresponds to +2 standard deviations above the least squares fit.

The permeability values in Table 5 and Figure 8 are reasonable and appropriate and are supported from several viewpoints:

- From 0 to 100 years, the crushed salt is assigned a permeability range of 2×10^{-19} m^2 to 10^{-12} m^2, representative of the combined test results from Hurtado et al. (1997), Case et al. (1987), and Zhang et al. (2007) for loosely consolidated ROM salt.

- From 100 to 200 years, the permeability range in Table 5 encompasses a wide range of possible outcomes, from a minimum permeability of 1.44×10^{-21} m^2 to a maximum permeability of 4.55×10^{-17} m^2. This range will produce a range of hydrologic responses for the ROM salt, from very "tight" to much "looser" in terms of brine and gas flows across the closure. This wide range has been chosen because of the uncertainties in emplacement of the ROM salt.

- From 200 to 10,000 years, the permeability range in Table 5 represents the response of fully compacted salt, with a minimum permeability of 4.46×10^{-22} m^2 and a maximum permeability of 1.47×10^{-17} m^2. This range of values is purposefully greater than the range for intact halite in PA, which is 10^{-24} m^2 to 10^{-21} m^2. The consolidation mechanisms for moistened versus dry crushed salt are different and can lead to different degrees of interconnected porosity and permeability for a given effective porosity. In this situation, the very low permeability of intact salt may not be attained for thousands of years by the ROM salt.

- After 100 years, the range of permeability in Table 5 is similar to the permeability range for material DRZ_PCS in the PABC-2009, which is 2×10^{-21} m^2 to 1×10^{-17} m^2 (Clayton et al. 2010), as discussed in Section 5.2 of this memorandum. The ranges of permeability after 100 years are therefore consistent with the expected response for a healed DRZ above and below a panel closure, as represented in PABC-2009.

5.1.3 Residual Brine Saturation and Residual Gas Saturation of ROM Salt

The residual gas saturation is the degree of gas saturation necessary to create an incipient interconnected pathway for a porous material to be permeable to gas. The residual gas saturation for all materials in the original shaft seal model, including crushed salt, was defined for the CCA (DOE, 1996, Appendix PAR, Parameter 14). The residual gas saturation was based on a literature review for consolidated geologic materials, concrete, and asphalt, and on professional judgment. Similarly the residual brine saturation for all shaft seal materials, including crushed salt, was defined for the CCA based on a literature review and on professional judgment (DOE, 1996, Appendix PAR, Parameter 15). The residual brine saturation and residual gas saturation of the ROM salt in the PCS will use the same distributions as the corresponding parameters for the crushed salt component of the shaft seals. These distributions are summarized in Table 6.

Table 6. Residual brine saturation and residual gas saturation of the ROM salt

Parameter	Distribution
PCS_T1:SAT_RBRN PCS_T2:SAT_RBRN PCS_T3:SAT_RBRN	Cumulative distribution: **Probability Value** 0.0 0.0 0.5 0.2 1.0 0.6
PCS_T1:SAT_RGAS PCS_T2:SAT_RGAS PCS_T3:SAT_RGAS	Uniform distribution: Minimum value: 0.0 Maximum value: 0.4

5.1.4 Relative Permeability Model and Capillary Pressure Model for ROM Salt

Several two phase flow models have been implemented in the BRAGFLO code, and the values of the parameters RELP_MOD and CAP_MOD define the relative permeability model and the capillary pressure model for a material, respectively. Most materials mapped to the BRAGFLO grid use a modified Brooks-Corey model for relative permeability, with the exception of the anhydrite Marker Beds and Anhydrite Layers a and b (DOE, 2009, Table PA-4), which switch between the Brooks-Corey and Van Genuchten models for relative permeability. The two phase flow model for the ROM salt will also use the modified Brooks-Corey model, which corresponds to relative permeability model number 4 (i.e., RELP_MOD = 4) (DOE, 2009, footnote to Table PA-4) and use capillary pressure model number 2 (i.e., CAP_MOD = 2), which has a fixed maximum capillary pressure. The choice of these models is independent of the timing of the consolidation process. Table 7 summarizes these values.

Table 7. Relative permeability model and capillary pressure model for the ROM salt

Parameters	Value
PCS_T1:RELP_MOD PCS_T2:RELP_MOD PCS_T3:RELP_MOD	4 (a modified Brooks –Corey model)
PCS_T1:CAP_MOD PCS_T2:CAP_MOD PCS_T3:CAP_MOD	2 (fixed maximum capillary pressure)

5.1.5 Other Two Phase Flow Parameters

Table 8 identifies seven parameters for the relative permeability and capillary pressure models for the ROM salt. All WIPP PA materials use the same values for KPT, PC_MAX, and PO_MIN. The crushed salt materials and concrete-related materials for the original shaft seal model use the same values and distributions for the COMP_RCK, PCT_A, PCT_EXP, and PORE_DIS parameters shown in Table 8. The values or distribution in Table 8 will be used for the ROM salt, independent of the time period.

Table 8. Two phase flow parameters for the ROM salt

Parameter	Description	Type	Value
COMP_RCK	Bulk Compressibility	Constant	8.0×10^{-11} Pa^{-1}
KPT	Flag for permeability determined threshold	Constant	0.0 (dimensionless)
PO_MIN	Minimum brine pressure for capillary model KPC=3	Constant	1.01325×10^{5} Pa
PC_MAX	Maximum allowable capillary pressure	Constant	1×10^{8} Pa
PCT_A	Threshold pressure linear parameter	Constant	0.56 Pa
PCT_EXP	Threshold pressure exponential parameter	Constant	-0.346 (dimensionless)
PORE_DIS	Brooks-Corey pore distribution parameter	Cumulative distribution	**Probability Value** 0.0 0.11 0.5 0.94 1.0 8.1

5.2 Hydrologic and Pore Compressibility Parameters of the DRZ Surrounding the ROMPCS

5.2.1 Porosity and Permeability of the DRZ

Initially it is expected that the DRZ around the PCS will be no different from that around the disposal rooms, since there will be only very small back stress from the consolidating ROM salt. Calculations for closure of panel entries and consolidation of the ROM salt have been performed for two bounding cases: (1) ROM salt that is emplaced and compacted to 20% porosity (80% fractional density), and (2) ROM salt that is emplaced without compaction to 35% porosity (65% fractional density) (Herrick 2012). The results of these calculations demonstrate that the time dependent backstress does not become appreciable until approximately 200 years after emplacement. While the back stress is low, the state of the DRZ surrounding the PCS will be similar to the state of the DRZ surrounding the disposal rooms, and it is appropriate to maintain the same ranges of DRZ porosity and DRZ permeability above and below the PCS as those around the disposal rooms during the first 200 years. Thus, the porosity of DRZ surrounding the PCS lies between 0.0039 and 0.0548 for the first 200 years (i.e. the same porosity range prescribed for material DRZ_1 in the PABC-2009). The permeability of the DRZ surrounding the PCS has a range of $10^{-12.5}$ m^2 to $10^{-19.4}$ m^2 for the first 200 years.

After 200 years, back pressures will have built up to values of the order of 6 to 10 MPa, as shown in Figures 9 and 10. It has been shown by several authors that fractures in salt will heal rapidly under these levels of stress (e.g., IT Corporation, 1987 and Costin and Wawersik, 1980). For example, Costin and Wawersik state:

- Tensile fractures in salt will heal when subjected to nominal overburden pressures (10-35 MPa), to the extent that the resistance to crack propagation along the pre-existing fracture plane is approximately 70-80% of that through virgin material.
- The healing process takes place rapidly compared to the time scale over which mining or storage in salt occurs.
- The principal mechanism in healing appears to be creep of contact asperities along the fracture surface.

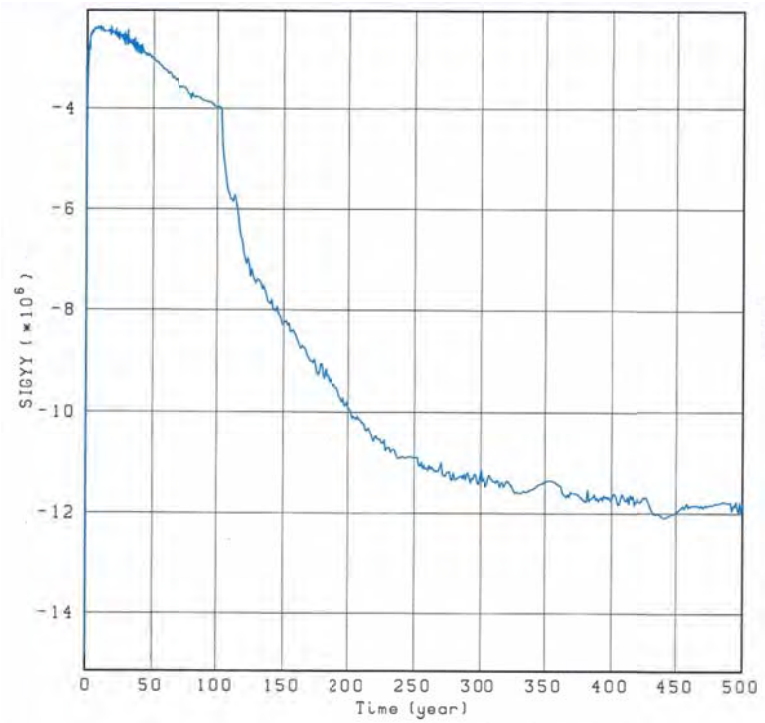

Figure 9. Vertical back stress on the roof of the panel entry for ROM salt with an initial emplacement porosity of 20% (fractional density of 80%) (Herrick 2012)

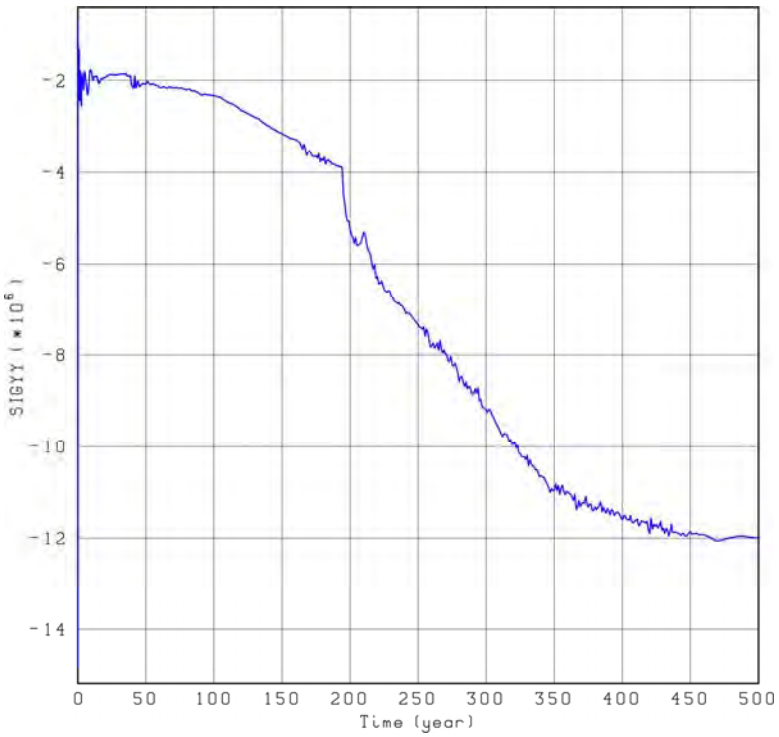

Figure 10. Vertical back stress on the roof of the panel entry for ROM salt with an initial emplacement porosity of 35% (fractional density of 65%) (Herrick 2012)

Given the values of back stress calculated for closures with some degree of emplaced compaction, and the rapid increase of stress even for the most extreme case of salt that is emplaced without compaction (see Figure 10), the back stress is expected to heal the DRZ directly above and below the ROMPCS, reducing its porosity and its permeability. It is then appropriate to assume that the porosity and permeability of the DRZ after 200 years will be equivalent to the state of the DRZ surrounding the Option D panel closure in the PA for CRA-2009 (DOE, 2009, Appendix PA) and in the PABC-2009. The porosity of the DRZ directly above and below the Option D panel closure in the PA for CRA-2009 and in the PABC-2009 has a minimum value of 0.0039 and a maximum value of 0.0548 at all times. The permeability of the DRZ directly above and below the Option D panel closure has a minimum value of 2×10^{-21} m^2 and a maximum value of 1×10^{-17} m^2 (DOE, 2009, Appendix PA, Sections PA-4.2.8.2 and PA-4.2.8.3). We have chosen that these ranges be used for the DRZ surrounding the ROMPCS after 200 years. Table 9 summarizes the ranges for porosity and permeability for the DRZ directly above and below the ROMPCS.

The selected porosity for the DRZ directly above and below the PCS is constant at all times. After 200 years, it is reasonable to expect that the healing of the DRZ caused by increasing back stress will reduce the DRZ porosity. A reduction in DRZ porosity should have minimal impact on the PCS-2012 PA because sensitivity calculations have demonstrated that PA results are insensitive to the porosity of a panel closure, and by extension to the porosity of the DRZ directly above and below the ROMPCS (DOE 2012, Response to EPA Question 1.2b).

Table 9. Porosity and permeability of the DRZ surrounding the PCS

Parameter	Value	Notes
DRZ_PCS_T1:POROSITY DRZ_PCS_T2:POROSITY DRZ_PCS_T3:POROSITY	0.0039 to 0.0548	Same range in the PA for CRA-2009 and the PABC-2009 as for the DRZ (material DRZ_1) around disposal rooms at all times.
DRZ_PCS_T1:PERMEABILITY DRZ_PCS_T2:PERMEABILITY	$10^{-19.4}$ m^2 to $10^{-12.5}$ m^2	Same permeability range in the PA for CRA-2009 and PABC-2009 for the DRZ (material DRZ_1) surrounding disposal rooms from 0 to 200 years.
DRZ_PCS_T3:PERMEABILITY	2×10^{-21} m^2 to 1×10^{-17} m^2	Same permeability range in the PA for CRA-2009 and PABC-2009 for the DRZ_PCS above and below the Option D panel closures after healing of the DRZ.

5.2.2 Two Phase Flow Parameters for Materials DRZ_PCS_T1 and DRZ_PCS_T2

During the first 200 years, while the back stress is low, the state of the DRZ surrounding the PCS will be similar to the state of the DRZ surrounding the disposal rooms, and it is appropriate to maintain the same values for two phase flow parameters for the DRZ directly above and below the ROMPCS as those for the DRZ around the disposal rooms. Table 10 identifies the values for the two phase flow parameters and their sources during the first 200 years.

5.2.3 Two Phase Flow Parameters for DRZ_PCS_T3 After 200 Years

After 200 years, the back pressure from the consolidated ROM salt is expected to heal the fractures in the DRZ directly above and below the PCS. In this state, the DRZ above and below the consolidated ROM salt is expected to have similar properties to the DRZ above and below the Option D monolith in the PA for the CRA-2009 and the PABC-2009. Therefore, the two phase flow parameters for the DRZ directly above and below the ROM salt shall be assigned the same values and distribution as the DRZ_PCS in the PA for CRA-2009 or the PABC-2009. Table 11 identifies the values for the two phase flow parameters and their sources after 200 years.

Table 10. Two phase flow parameters for the DRZ directly above and below the ROMPCS during the first 200 years

Parameter	Description	Value	Source
DRZ_PCS_T1:SAT_RBRN DRZ_PCS_T2:SAT_RBRN	Residual brine saturation	0.0	DOE, 2009, Table PA-3 for material DRZ_1
DRZ_PCS_T1:SAT_RGAS DRZ_PCS_T2:SAT_RGAS	Residual gas saturation	0.0	DOE, 2009, Table PA-3 for material DRZ_1
DRZ_PCS_T1:RELP_MOD DRZ_PCS_T2:RELP_MOD	Relative permeability model number	4 (modified Brooks-Corey model)	DOE, 2009, Table PA-4 for material DRZ_1
DRZ_PCS_T1:CAP_MOD DRZ_PCS_T2:CAP_MOD	Capillary pressure model number	1 (capillary pressure is unbounded)	DOE, 2009, Table PA-4 for material DRZ_1
DRZ_PCS_T1:KPT DRZ_PCS_T2:KPT	Flag for permeability determined threshold	0.0	Stein, SNL, ERMS 520524, Table 2
DRZ_PCS_T1:PO_MIN DRZ_PCS_T2:PO_MIN	Minimum brine pressure for capillary model KPC=3	1.01325×10^5 (Pa)	Stein, SNL, ERMS 520524, Table 2
DRZ_PCS_T1:PC_MAX DRZ_PCS_T2:PC_MAX	Maximum allowable capillary pressure	1.0×10^8 (Pa)	Stein, SNL, ERMS 520524, Table 2
DRZ_PCS_T1:PCT_A DRZ_PCS_T2:PCT_A	Threshold pressure linear parameter	0.0	DOE, 2009, Table PA-3 for material DRZ_1
DRZ_PCS_T1:PCT_EXP DRZ_PCS_T2:PCT_EXP	Threshold pressure exponential parameter	0.0	DOE, 2009, Table PA-3 for material DRZ_1
DRZ_PCS_T1:PORE_DIS DRZ_PCS_T2:PORE_DIS	Brooks-Corey pore distribution parameter	0.7	DOE, 2009, Table PA-3 for material DRZ_1

Table 11. Two phase flow parameters for the DRZ directly above and below the ROMPCS after 200 years

Parameter	Description	Value	Source
DRZ_PCS_T3:SAT_RBRN	Residual brine saturation	0.0	DOE, 2009, Table PA-3 for material DRZ_PCS
DRZ_PCS_T3:SAT_RGAS	Residual gas saturation	0.0	DOE, 2009, Table PA-3 for material DRZ_PCS
DRZ_PCS_T3:RELP_MOD	Relative permeability model number	4 (modified Brooks-Corey model)	DOE, 2009, Table PA-4 for material DRZ_PCS
DRZ_PCS_T3:CAP_MOD	Capillary pressure model number	1 (capillary pressure is unbounded)	DOE, 2009, Table PA-4 for material DRZ_PCS
DRZ_PCS_T3:KPT	Flag for permeability determined threshold	0.0	Stein, SNL, ERMS 520524, Table 2
DRZ_PCS_T3:PO_MIN	Minimum brine pressure for capillary model KPC=3	1.01325×10^5 (Pa)	Stein, SNL, ERMS 520524, Table 2
DRZ_PCS_T3:PC_MAX	Maximum allowable capillary pressure	1.0×10^8 (Pa)	Stein, SNL, ERMS 520524, Table 2
DRZ_PCS_T3:PCT_A	Threshold pressure linear parameter	0.0	DOE, 2009, Table PA-3 for material DRZ_PCS
DRZ_PCS_T3:PCT_EXP	Threshold pressure exponential parameter	0.0	DOE, 2009, Table PA-3 for material DRZ_PCS
DRZ_PCS_T3:PORE_DIS	Brooks-Corey pore distribution parameter	0.7	DOE, 2009, Table PA-3 for material DRZ_PCS

6.0 Summary

The DOE has submitted a planned change request to the EPA proposing that a revised panel closure design be approved for use in all WIPP waste panels. Panel closures are emplaced in the WIPP to protect workers during the operational phase of the facility. They are represented in PA because they are a significant physical feature of the repository. Long-term repository performance has been repeatedly shown to be insensitive to panel closure material properties. The revised panel closure design proposed by the DOE is comprised of 100 feet of run-of-mine salt with barriers at each end. A performance assessment named the PCS-2012 PA is planned to quantify regulatory compliance impacts resulting from the incorporation of the new closure design in the repository. PA materials, properties, and timings are developed to allow for modeling of the revised panel closure system in the PCS-2012. These parameter choices are reasonable values that will adequately represent the PCS within PA, and are based on sound science, modeling, and external data sources where available.

7.0 References

Ahrens, E.H., and F.D. Hansen. 1995. Large-Scale Dynamic Compaction Demonstration Using WIPP Salt: Fielding and Preliminary Results. Sandia National Laboratories. Albuquerque, NM. SAND95-1941.

Bechthold, W., E. Smailos, S. Heusermann ,T. Bollingerfehr, B Bazargan Sabet, T. Rothfuchs, P. Kamlot, J Grupa, S. Olivella, and F. D. Hansen. 2004. *Backfilling and Sealing of Underground Repositories for Radioactive Waste in Salt (BAMBUS II Project)*: final report. European Commission, Directorate General for Research, Office for Official Publications of the European Communities. Call No: EUR 20621 EN. Showcased in Research for Europe: Successful EU-funded projects by the Directorate General for Research.

Blanford, M.L., M.W. Heinstein, and S.W. Key. 2001. JAS3D: A Multi-Strategy Iterative Code for Solid Mechanics Analysis User's Instructions, Release 2.0. Sandia National Laboratories. ERMS 552358.

Brodsky, N.S., 1994. Hydrostatic and Shear Consolidation Tests With Permeability Measurements on Waste Isolation Pilot Plant Crushed Salt. Sandia National Laboratories. Albuquerque, NM. SAND93-7058.

Brodsky, N.S., F.D. Hansen, and T. Pfeifle. 1996. "Properties of Dynamically Compacted WIPP Salt." *Proceedings of the 4th International Conference on the Mechanical Behavior of Salt, Montreal, Quebec, Canada, June 17-18, 1996.* Sandia National Laboratories. Albuquerque, NM. SAND96-0838C.

Callahan G.D. and K.L. DeVries. 1991. Analyses of Backfilled Transuranic Wastes Disposal Rooms. Sandia National Laboratories. SAND91-7052.

Callahan, G.D., M .C. Loken, L.L. Van Sambeek, R. Chen, T.W. Pfeifle, J.D. Nieland, and F.D. Hansen. 1995. Evaluation of Potential Crushed-Salt Constitutive Models. Sandia National Laboratories. Albuquerque, NM. SAND95-2143.

Callahan, G.D. 1999. Crushed Salt Constitutive Model. Sandia National Laboratories, SAND98-2680.

Camphouse, R.C., Clayton, D.J., Kicker, D.C., and Pasch, J.J. 2011. Summary Report for the AP-151 (PC3R) Performance Assessment, Revision 1. Sandia National Laboratories, Carlsbad, NM. ERMS 555489.

Case, John B., Peter C. Kelsall, and James L. Withiam. 1987. *Laboratory Investigation of Crushed Salt Consolidation.* 28th US Symposium on Rock Mechanics, Tucson, Arizona, 29 June – 1 July 1987.

Clayton, D.C., Camphouse, R. C., Garner, J. W., Ismail, A. E., Kirchner, T. B., Kuhlman, K. L., and Nemer, M. B.. 2010. Summary Report of the CRA-2009 Performance Assessment Baseline Calculation, Revision 1. Sandia National Laboratories. Carlsbad, New Mexico, ERMS 553039.

Costin, L.S. and W. R. Wawersik. 1980. Creep Healing of Fractures in Rock Salt. Sandia National Laboratories. SAND80-0392.

DOE (U.S. Department of Energy). 1996. Title 40 CFR Part 191 Compliance Certification Application for the Waste Isolation Pilot Plant. DOE/CAO-1996-2184. U.S. Department of Energy, Waste Isolation Pilot Plant, Carlsbad Area Office. Carlsbad, NM.

DOE (U.S. Department of Energy). 2004. Title 40 CFR Part 191 Compliance Recertification Application for the Waste Isolation Pilot Plant. DOE/WIPP 2004-3231, 10 vols. U.S. Department of Energy, Carlsbad Field Office. Carlsbad, NM.

DOE (U.S. Department of Energy). 2009. Title 40 CFR 191 Parts B and C Compliance Recertification Application. DOE/WIPP-09-3424. Carlsbad Field Office. Carlsbad, New Mexico.

DOE (U.S. Department of Energy), 2011. Panel Closure System Design, Planned Change Request to the EPA 40 CFR Part 194 Certification of the Waste Isolation Pilot Plant. U.S. Department of Energy, Carlsbad Field Office. Carlsbad, New Mexico.

DOE (U.S. Department of Energy), 2012. Response to First Set of EPA Questions to DOE, December 22, 2011. Letter from Mr. Juan Franco, Manager, Carlsbad Area Field Office, U.S. Department of Energy, to Mr. Jonathan Edwards, Director, Radiation Protection Division, U.S. Environmental Protection Agency, dated April 17, 2012.

Dunagan, S. C. 2003. Complementary Cumulative Distribution Functions (CCDFs) for the Technical Baseline Migration (TBM), Revision 0. Sandia National Laboratories, Carlsbad, NM. ERMS 525707.

EPA (U.S. Environmental Protection Agency). 1998. Criteria for the Certification and Re-Certification of the Waste Isolation Pilot Plants Compliance with the 40 CFR Part 191 Disposal Regulations: Certification Decision; Final Rule, *Federal Register*, Vol. 63, No. 95, pp. 27353-27406. U.S. Environmental Protection Agency, Office of Air and Radiation, Washington, D.C.

Hansen, C. W. 2002. Analysis Report for the Panel Closure Impact Assessment. Sandia National Laboratories, Carlsbad, NM. ERMS 523935.

Hansen, F.D. 2003. The Disturbed Rock Zone at the Waste Isolation Pilot Plant. Sandia National Laboratories. Albuquerque, NM. SAND2003-3407.

Herrick, C.G. 2012. JAS3D Calculations Performed in Support of the PCS-2012 PA Parameter Selections. Sandia National Laboratories, Carlsbad, NM.

Hurtado, L.D., Knowles, M.K., Kelly, V.A., Jones, T.L., Ogintz, J.B., and T.W. Pfeifle. 1997. WIPP Shaft Seal System Parameters Recommended to Support Compliance Calculations. Sandia National Laboratories. Albuquerque, New Mexico. SAND97-1287.

IT Corporation. 1987. Laboratory Investigation of Crushed Salt Consolidation and Fracture Healing. Prepared for Office of Nuclear Waste Isolation. BMI/ONWI-631.

MacKinnon R. and G. Freeze, 1997. Supplemental Summary of EPA-Mandated Performance Assessment Verification Test (All Replicates) and Comparison with the Compliance Certification Application Calculations, Sandia National Laboratories, Carlsbad, NM. ERMS 414880. (EPA Docket A-93-02, II-G-28.)

Pettigrew and Associates. 1993. *Sieve Analysis on Salt Backfill Sample #1* and *Sieve Analysis on Salt Backfill Sample #2*. Carlsbad, New Mexico.

RockSol Consulting Group, Inc. 2006. Further Assessment of the Short-term Stability of the 12 Foot Explosion Isolation Wall. Report prepared for Washington TRU Solutions, LLC.

Rothfuchs, Tilmann, and Klaus Wieczorek. 2010. *Backfill Compaction and EDZ Recovery*. US-German Workshop on Salt Repository Research, May 25-28, 2010, Jackson, Mississippi.

Sjaardema, G.D., and R.D. Krieg. 1987. A Constitutive Model for the Consolidation of WIPP Crushed Salt and It's Use in Analyses of Backfilled Shaft and Drift Configurations. Sandia National Laboratories. Albuquerque, NM. SAND87-1977.

Spiers, C.J., J.L. Urai, and G.S. Lister. 1988. "The Effect of Brine (Inherent or Added) on Rheology and Deformation Mechanisms in Salt Rock," *The Mechanical Behavior of Salt, Proceedings of the Second Conference, Federal Institute for Geosciences and Natural Resources, Hanover, Federal Republic of Germany, September 24-28, 1984*, 89 to 102. H.R. Hardy, Jr. and M. Langer (eds.). Clausthall-Zellerfeld, Germany: Trans Tech Publications.

Van Sambeek, L.L., T. J. Eyerman, and F. D. Hansen. 1995. Case Studies of Sealing Methods and Materials Used in the Salt and Potash Mining Industries. Sandia National Laboratories. Albuquerque, NM. SAND95-1120.

Vugrin, E.D. and S.C. Dunagan. 2006. Analysis Package for the Impact Assessment of the Redesigned Panel Closure System, Rev. 0. Sandia National Laboratories. Carlsbad, NM. ERMS 543865.

Vugrin, E., and S. Wagner. 2006. Panel Closure Summary Report. Sandia National Laboratories. Carlsbad, NM. ERMS 544802.

Weatherby, J. R. 1989. Finite Element Analysis of TRU Storage Rooms Filled With Waste and Crushed Salt. Sandia National Laboratories Internal Memorandum to B. M. Butcher, Division 6332, Albuquerque, NM.

Zhang, Chun-Liang, Tilman Rothfuchs, and Johannes Droste, 2007. *Post-tests on thermo-mechanically compacted salt backfill.* The Mechanical Behavior of Salt – Understanding of THMC Processes in Salt, Wallner, Lux, Minkley and Hardy, Jr., Editors.